Structural study of one-phase microemulsions

ARTICLE *in* THE JOURNAL OF PHYSICAL CHEMISTRY · DECEMBER 1986

Impact Factor: 2.78 · DOI: 10.1021/j100283a015

7 AUTHORS, INCLUDING:

Jorge E. Puig
University of Guadalajara
193 PUBLICATIONS **2,902** CITATIONS

SEE PROFILE

Structural Study of One-Phase Microemulsions

D. S. Rushforth, M. Sanchez-Rubio, L. M. Santos-Vidals,

Departmento de Química, Centro de Investigacion y Estudios Avanzados, I.P.N., 07000 Mexico, D.F.

K. R. Wormuth, E. W. Kaler,*

Department of Chemical Engineering, BF-10, University of Washington, Seattle, Washington 98195

R. Cuevas, and J. E. Puig

Facultad de Ciencias Químicas, Universidad de Guadalajara, 44430 Guadalajara, Jal., Mexico
(Received: May 5, 1986; In Final Form: August 1, 1986)

Several microemulsion microstructures were identified in the one-phase region of the sodium dodecyl sulfate/1-butanol/toluene/2.5 wt % NaCl brine system by quasielastic light scattering, conductivity, viscosity, and steady-state fluorescence-probe measurements. At high ratios of water to oil, microemulsions are aqueous solutions of oil-swollen micelles; at low ratios of water to oil, microemulsions are oleic solutions of water-swollen inverted micelles; near the three-phase region, where the microemulsion takes up substantial amounts of both water and oil, the structure is a bicontinuous interpenetrating network of water and oil domains separated by surfactant layers. There is also a large excluded region for droplets where small hydrated surfactant aggregates solvated with alcohol molecules are dispersed in an oleic medium, and a small region, near the 2-phase boundary, where the structure is unknown.

Introduction

Microemulsions are thermodynamically stable, isotropic, microstructured fluid phases containing substantial amounts of oil and water (or brine), and surfactant. Increasing attention is being paid to these phases because of their unusual physicochemical properties and some potentially large-scale applications of commercial importance such as detergency, enhanced oil recovery, phase-transfer catalysis, and photochemical and polymerization reactions.[1-7] Much of the effort has been directed toward elucidating the kinds of fluid microstructures present in microemulsions and how they change as the relative amounts of oil and water vary, particularly for microemulsions that incorporate substantial amounts of oil and water. Microemulsion structure has been investigated by a variety of techniques such as NMR spectroscopy, electrical conductivity, tracer self-diffusion measurements, quasielastic light scattering, small-angle scattering, and fluorescence spectroscopy.[8-19]

The usual situation is that when the volume fraction of dispersed oil is small, the microemulsion is a water-continuous solution of micelles swollen with oil, and that when the volume fraction of dispersed water is small the microemulsion is an oleic solution of inverted micelles swollen with water. However, the structures of microemulsions containing almost equal amounts of oil and water or with high surfactant content are not well established. Several structures have been proposed for such microemulsions including bicontinuous or lamellar ones, and some systems may be simply cosolubilized solutions without microstructure.[20-22]

In a previous paper[19] we reported preliminary conductance and fluorescence-probe measurements of one-phase microemulsions made of sodium dodecyl sulfate (SDS), 1-butanol (NBA), toluene, and 2.5 wt % NaCl brine. We detected three patterns of microemulsion conductance as a function of toluene volume fraction and an interesting minimum in the pyrene excimer formation as a function of brine volume fraction. Here we present the results of extensive conductance, quasielastic light scattering, fluorescence-probe, and viscosity measurements in the whole one-phase region of the pseudoternary phase diagram of the SDS/NBA/toluene/2.5 wt % NaCl brine system and infer from them a picture of the structure of the microemulsion. Our results indicate that there are, at least, three types of microemulsion structures: water continuous (containing swollen micelles), oil continuous (containing swollen inverted micelles), and bicontinuous. There is also a large excluded region for droplets in which the system probably consists of small hydrated soap aggregates solvated by alcohol dispersed in an oleic medium, and a small region near the 2 phase boundary where the structure is not yet known.

Experimental Section

Sodium dodecyl sulfate (SDS) was specially pure (>99%) from Merck or BDH (Biochemical Grade). Toluene and 1-butanol (NBA) were 99% pure from Phillips Petroleum and Baker

(1) *Microemulsions. Theory and Practice*, Prince, L. M., Ed.; Academic: New York, 1977.
(2) Reed, R. L.; Healy, R. N. in *Improved Oil Recovery by Surfactant and Polymer Flooding*, Shah, D. O., Schechter, R. S., Eds.; Academic: New York; 1977 p 383.
(3) Thomas, J. K. *Chem. Rev.* **1980**, *80*, 283.
(4) Fendler, J. H.; Fendler, E. J. *Catalysis in Micellar and Macromolecular Systems*; Academic: New York, 1975.
(5) *Micellization, Solubilization and Microemulsions*, Mittal, K. L., Ed.; Plenum: New York, 1977.
(6) *Microemulsions*, Robb, I. D., Ed.; Plenum: New York, 1982.
(7) Jayakrishnan, A.; Shah, D. O. *J. Polym. Sci., Polym. Lett. Ed.* **1984**, *22*, 31.
(8) Biais, J.; Clin., B.; Lalanne, P.; Lemanceau, B. *J. Chim. Phys.* **1977**, *74*, 11.
(9) Lindman, B.; Stilbs, P.; Moseley, M. E. *J. Colloid Interface Sci.* **1981**, *83*, 569.
(10) Lagües, M.; Ober, R.; Taupin, C. *J. Phys. Lett.* **1978**, *39*, L-487.
(11) Bennett, K. E.; Hatfield, J. C.; Davis, H. T.; Macosko, C. W.; Scriven, L. E. In *Microemulsions*, Robb, I. D., Ed.; Plenum: New York, 1981; p 65.
(12) Chen, S. J.; Evans, D. F.; Ninham, B. W. *J. Phys. Chem.* **1984**, *88*, 1631.
(13) Lindman, B.; Kamenka, N.; Karthopoulis, T.; Brun, B.; Nilsson, P. *J. Phys. Chem.* **1980**, *84*, 2484.
(14) Zulauf, M.; Eicke, H. F. *J. Phys. Chem.* **1979**, *83*, 480.
(15) Cazabat, A. M.; Langevin, D.; Pouchelon, A. *J. Colloid Interface Sci.* **1980**, *73*, 1.
(16) Kaler, E. W.; Davis, H. T.; Scriven, L. E. *J. Chem. Phys.* **1983**, *79*, 5685.
(17) Auvray, L.; Cotton, J. P.; Ober, R.; Taupin, C. *J. Phys.* **1984**, *45*, 913.
(18) Lianos, P.; Lang, J.; Zana, R. *J. Phys. Chem.* **1982**, *86*, 4809.
(19) Sanchez-Rubio, M.; Santos-Vidals, L. M.; Rushforth, D. S.; Puig, J. E. *J. Phys. Chem.* **1985**, *89*, 411.
(20) Scriven, L. E. *Nature (London)* **1976**, *263*, 123. In *Micellization, Solubilization, and Microemulsions*, Mittal, K. L., Ed., Vol. 2; Plenum: New York, 1977; p 877.
(21) Shah, D. O.; Bansal, V. K.; Chan, K.; Hsieh, N. C. In *Improved Oil Recovery by Surfactant and Polymer Flooding*, Shah, D. O., Schechter, R. S., Eds., Academic: New York, 1977; p 293.
(22) Bellocq, A. M.; Fourche, G. *J. Colloid Interface Sci.* **1980**, *78*, 275.

0022-3654/86/2090-6668$01.50/0

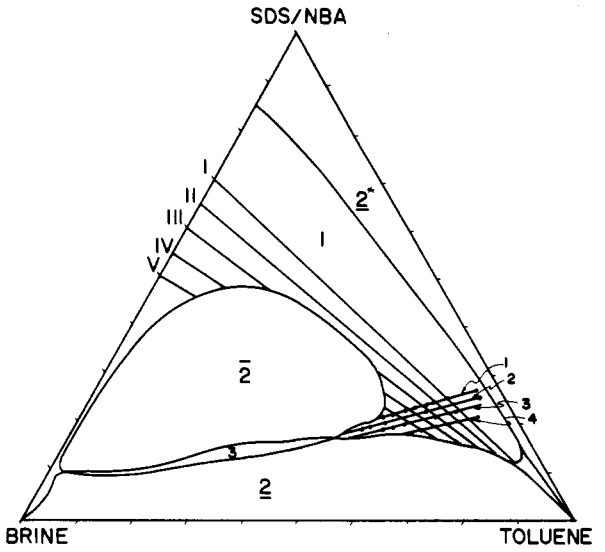

Figure 1. Pseudoternary phase diagram (in weight percent) at 25 °C. The weight ratio of NBA to SDS is 2. Lines in diagram indicate dilution paths investigated by QLS and fluorescence spectroscopy. Lines I–V are oil-dilution paths; lines 1–4 are water-dilution paths. Other notation is explained in the text.

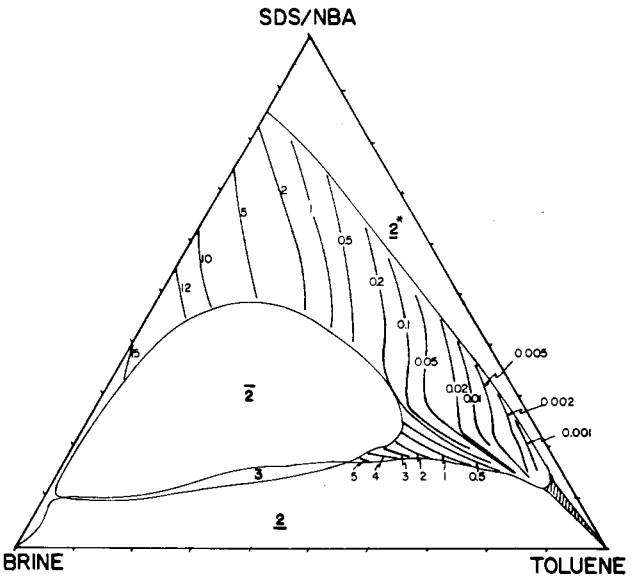

Figure 2. Lines of isoconductivity in the one-phase region of the pseudoternary phase diagram.

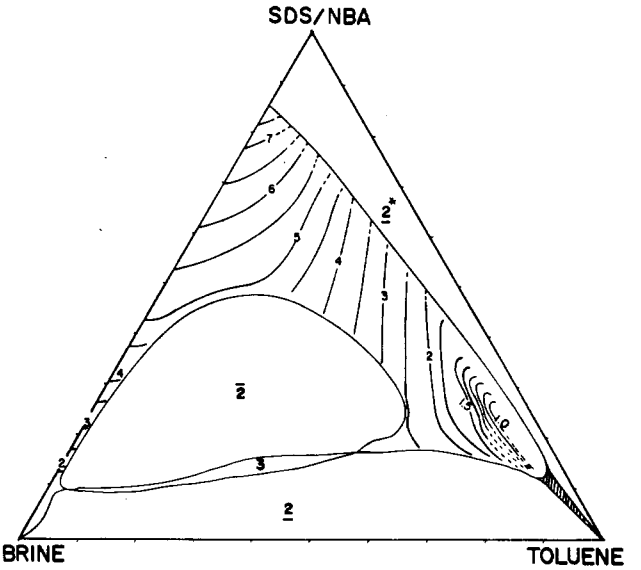

Figure 3. Lines of isoviscosity in the one-phase region of the pseudoternary phase diagram.

Chemical Co., respectively, or from Aldrich Chemical Co. Water was doubly distilled, with conductivity less than 1 μS cm^{-1}. Pyrene was scintillation grade from Baker Chemical Co.; it was recrystallized three times from ethanol before use. Sodium chloride, ACS grade from Fisher Scientific or Mallincrodt Inc., was dried in a vacuum oven before use.

Samples were prepared by weighing all the components in frozen glass ampules which were sealed to prevent evaporation, gently hand-shaken, and equilibrated in a constant-temperature water bath before making any measurements. The samples were maintained and all measurements made at 25.0 ± 0.05 °C. The criterion for equilibrium was the reproducibility of the number and volumes of phases in shaking-and-standing cycles. In some cases, samples were made by diluting one-phase stock samples of 2.5 wt % NaCl brine and active mixture with toluene. The active mixture was one part by weight SDS and two parts by weight NBA. To convert the data from weight percent to volume fraction, a value of 1.02 g/cm^3 for the surfactant density was used. This value was obtained by measuring the densities of one-phase samples of varying compositions of brine and active mixture (NBA/SDS = 2), and then extrapolating to zero brine concentration.

The quasielastic light scattering (QLS) apparatus consisted of a laser light source (2-W argon ion, Spectra Physics Model 165), a thermostated Malvern sample holder with refractive index matching bath, and a Thorn/EMI phototube detector. A Langley-Ford Model 1096 correlator calculated the autocorrelation function of the scattered intensity fluctuations, which was analyzed by the method of cumulants.[23] The measured autocorrelation functions decayed as single exponentials except for samples near the 2 phase boundary when measured at low scattering angles. The scattered light was never depolarized, so multiple scattering effects were unimportant. The samples were filtered by gravity through 0.22-μm Millipore filters into 1-cm-diameter cells.

Conductance was measured with a Metrohm conductance meter Model 644 and a Jones-type cell (cell constant of 28.03 cm^{-1}) or an immersion cell (0.46 cm^{-1}). All measurements were made at frequencies of 1000 or 2000 Hz. Viscosities were measured with a calibrated Ubbelhode viscometer immersed in a water bath. Uncorrected fluorescence spectra were taken with an AMINCO SPF-500 Ratio spectrofluorometer or with a Perkin-Elmer LS-5 Luminescence spectrometer. The excitation wavelength was 337 nm. The intensities reported here were measured at wavelengths of 395 nm, where molecular pyrene emits, and 466 nm, where the excimer emits,[24] with emission and excitation bandpasses of 2 nm.

(23) Koppel, D. E. *J. Chem. Phys.* **1972**, *57*, 4814.

Results

The pseudoternary phase diagram in weight percent at 25 °C is shown in Figure 1 (cf. ref 25). The phase diagram is defined by a constant alcohol/surfactant weight ratio of 2. The different regions are indicated with a mnemonic notation that gives the number of phases in equilibrium and the location of the surfactant-rich phase: 2 indicates a two-phase region where a lower microemulsion phase is in equilibrium with an oil-rich one; $\bar{2}$ denotes a two-phase region where an upper microemulsion phase and a brine-rich phase are in equilibrium; 3 represents a three-phase region where the microemulsion is the middle phase; 2* symbolizes a biphasic region where the phase is a surfactant-rich white precipitate that shows birefringence in the polarizing microscope; and 1 denotes the one-phase region where the attention of this work is concentrated. The dots on the numbered lines drawn on the phase diagram represent the compositions of the samples investigated by QLS or by fluorescence spectroscopy.

(24) Turro, N. *Modern Molecular Photochemistry*; Benjamin/Cummings: San Francisco, 1978.

(25) Bellocq, A. M.; Biais, J.; Chin, B.; Gelot, A.; Lalanne, P.; Lemanceau, B. *J. Colloid Interface Sci.* **1980**, *74*, 311.

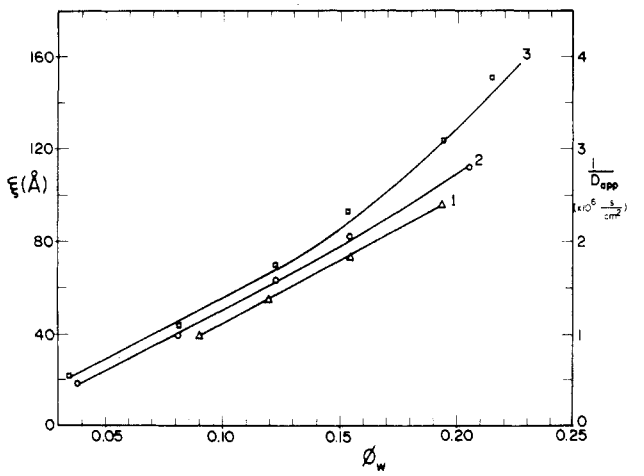

Figure 4. Reciprocal of the apparent diffusion coefficient, $1/D_{app}$, and the characteristic length, ξ, vs. brine volume fractions, ϕ_w, along paths 1, 2, and 3.

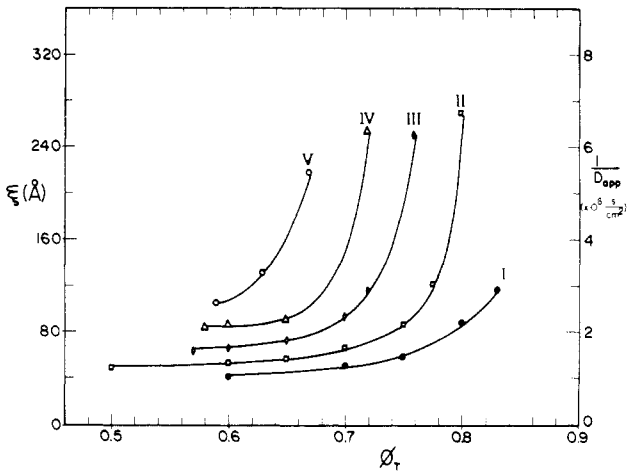

Figure 5. Reciprocal of the apparent diffusion coefficient and characteristic length vs. toluene volume fraction, ϕ_T, along paths I through V.

Figure 2 reports lines of isoconductivity. Microemulsion conductivity is highest at the brine-rich corner and falls as the composition moves away from it. Conductivity increases again as the microemulsion composition approaches the three-phase region and then decreases as the toluene-rich corner is approached. In this region, conductivity has its lowest value.

Lines of isoviscosity are shown in Figure 3. Microemulsion viscosity is low in the whole one-phase region. The highest viscosity (~8 cP) was detected at the upper (surfactant-rich) corner of the phase diagram.

Plots of the reciprocal of the apparent diffusion coefficient, $1/D_{app}$, and the characteristic length, ξ, measured along lines 1, 2, and 3 (see Figure 1), vs. brine volume fraction, ϕ_w, are displayed in Figure 4. In the absence of interactions, $D_{app} = D_0$, where D_0 is the z-averaged intrinsic mutal diffusion coefficient of the particles. D_0 is inversely proportional to the hydrodynamic radius, R_h, as

$$\frac{1}{D_0} = \left[\frac{6\pi\eta}{kT}\right] R_h$$

where k is the Boltzmann constant, T the temperature, and η the viscosity of the medium. However, as the concentration of particles increases, the interpretation of D_{app} becomes ambiguous due to the effects of thermodynamic and hydrodynamic interactions. As discussed below, we define a characteristic length, ξ, as

$$\frac{1}{D_{app}} = \left[\frac{6\pi\eta}{kT}\right] \xi$$

In dilute dispersions, $\xi \sim R_h$, and at low ϕ_w (Figure 4), ξ corresponds to the dimension of micellar-sized structures. As ϕ_w increases, ξ grows linearly along paths 1 and 2, but curves upward for ϕ_w greater than $\cong$0.1 along path 3.

Figure 5 reports QLS data along paths with a constant ratio of active mixture to brine diluted with toluene (lines I to V in Figure 1). Along paths I and II, at toluene volume fractions (ϕ_T) smaller than approximately 0.5, the scattered light is extremely weak. This suggests the absence of micellar-sized structure. Above $\phi_T \cong 0.5$, the signal is stronger and analysis yields micellar-sized characteristic lengths. At larger ϕ_T, $1/D_{app}$ and ξ diverge dramatically as the phase boundary (2) is approached. A different phase boundary (2*) was approached along path I, and a weaker ξ divergence results.

The presence of interparticle interactions, polydispersity, nonspherical structures, or critical fluctuations leads to scattering that depends on the magnitude of the scattering vector q

$$q = \frac{4\pi n}{\lambda} \sin(\theta/2)$$

where n is the refractive index of the solution, λ the wavelength of light, and θ the scattering angle. The scattering from samples along path 1 shows no dependence upon the scattering vector, q. A weak dependence of D_{app} upon q is found only for the last samples of paths 2 and 3 before phase separation (Figure 6). Along the toluene dilution paths (lines I to V), the q dependence of $1/D_{app}$ is also significant only for the last samples before phase separation (Figure 6). There is no q dependence of D_{app} along path I. The autocorrelation functions of the last samples of paths III and V (near the phase boundary) at low q were not single exponential decays.

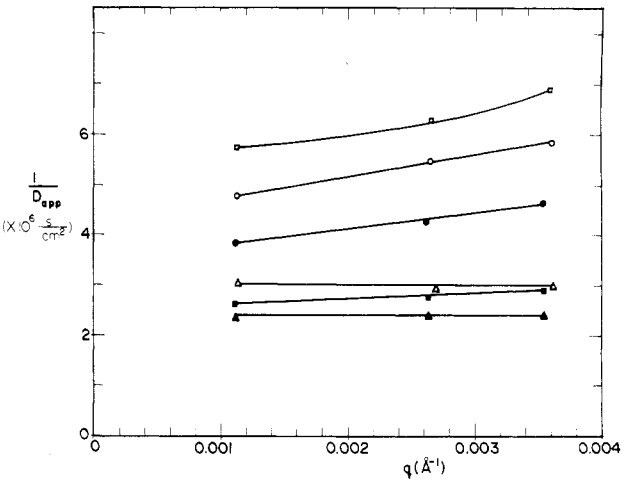

Figure 6. Reciprocal of the apparent diffusion coefficient vs. scattering vector, q, for the following samples: □, line III, $\phi_T = 0.76$; ○, line V, $\phi_T = 0.67$; ●, line 3, $\phi_W = 0.27$; △, line I, $\phi_T = 0.82$; ■, line 2, $\phi_W = 0.23$; ▲, line 1, $\phi_W = 0.21$.

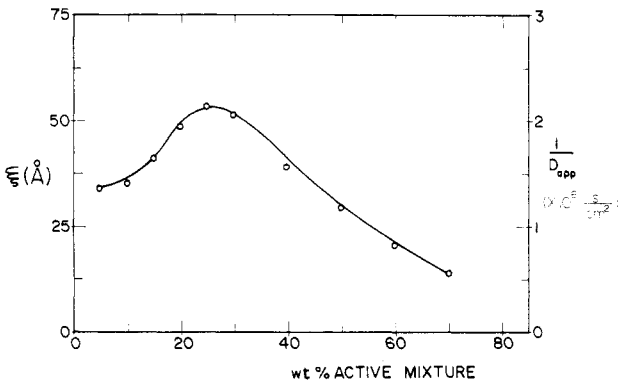

Figure 7. Reciprocal of the apparent diffusion coefficient and characteristic length vs. weight percent active mixture in toluene-free samples.

QLS measurements were also taken of samples along the active mixture/brine edge of the phase diagram (Figure 7). ξ is a

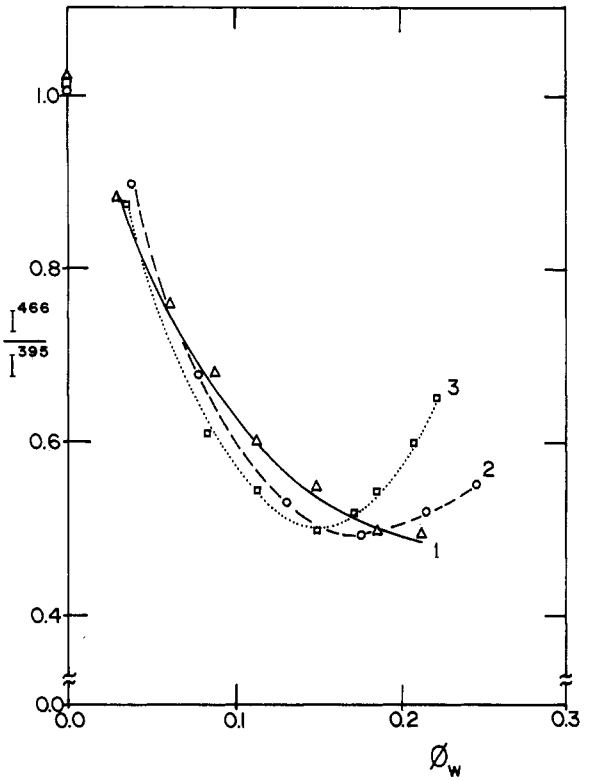

Figure 8. Ratio of pyrene excimer emission intensity measured at 466 nm to pyrene emission intensity measured at 395 nm (I^{466}/I^{395}) as a function of brine volume fraction along paths 1, 2, and 3.

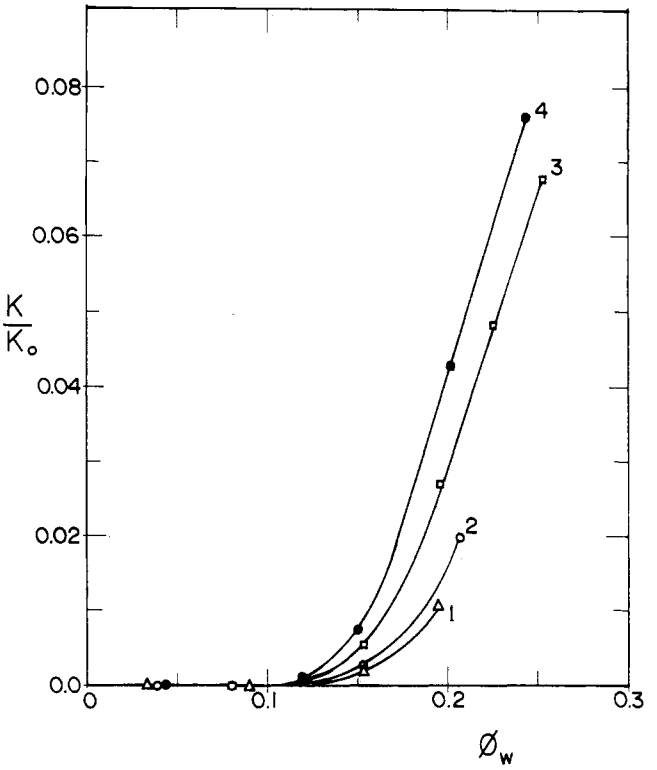

Figure 9. Ratio of microemulsion and brine conductivities, K/K_0, vs. brine volume fraction along paths 1 through 4.

maximum at 25 wt % active mixture. Above 60 wt % active mixture, ξ is small which indicates there is little fluid structure; ξ depends little on q along this path.

The results of fluorescence probe measurements as a function of ϕ_w along lines 1, 2, and 3 are reported as the ratio of the intensity at 466 nm to that at 395 nm, I^{466}/I^{395} (Figure 8). The pyrene concentration was 5×10^{-3} mol/L of toluene. The ratio of I^{466}/I^{395} is a relative measure of excimer formation in the microemulsion.[26,27] For comparison, the value of I^{466}/I^{395} in pure toluene is also shown. A minimum in excimer formation is observed in lines 2 and 3 but not in line 1. The position of the minimum is independent of pyrene concentration, at least in the range examined.[26]

Figure 9 is a plot of the ratio of microemulsion and brine conductivities, K/K_0, vs. brine volume fraction for microemulsions along paths 1 to 4. At high ϕ_w, conductivity grows almost linearly as ϕ_w increases. Moreover, it increase dramatically at finite brine volume fraction ($\phi_w \sim 0.12$), suggesting a percolation threshold.

Figure 10 reports the conductivity of microemulsions along lines I to V as ϕ_T varies. Three patterns of conductivity are observed: along line I conductivity decreases as ϕ_T increases; along lines IV and V conductivity increases as ϕ_T increases; and along lines II and III conductivity goes through a minimum.

Discussion and Conclusions

Macroscopic properties of microemulsions like viscosity, electrical conductivity, excimer formation, and phase behavior must be related to fluid microstructure. Techniques like those used here can provide valuable information about structural behavior of micellar solutions and microemulsions by determining the nature of the continuous phase and detecting phase-inversion phenomena and percolation behavior.

Conductance measures the ability of ions in aqueous domains to move from one electrode to another under the influence of an electrical field. Thus, it is expected that water-continuous microemulsions ought to display fairly high conductivity in contrast

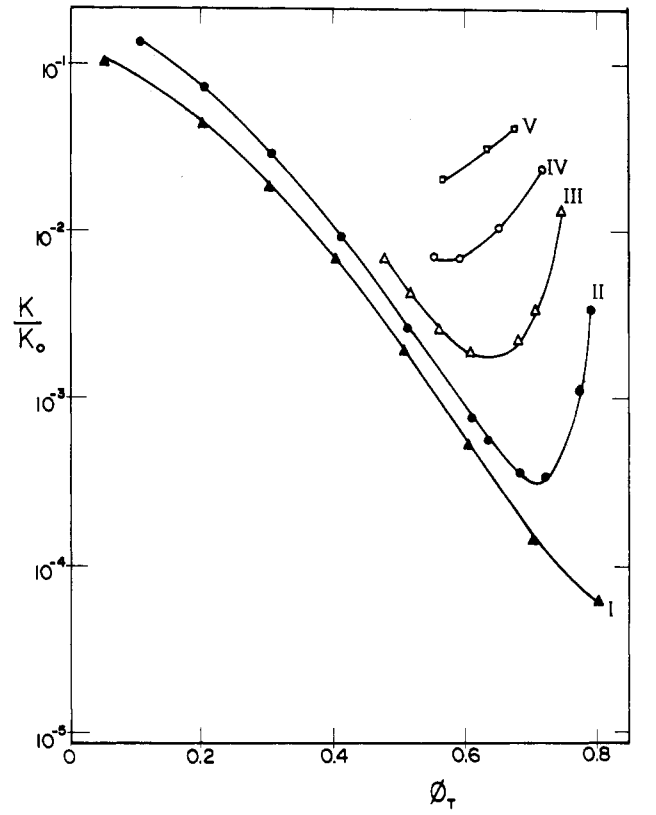

Figure 10. Ratio of microemulsion and brine conductivities, K/K_0, vs. toluene volume fraction along paths I through V.

to oil-continuous ones which should be poorly conducting or nonconducting. Excimer formation measures the ease of movement of fluorescent probe molecules in a micellar or a microemulsion structure. In particular, pyrene excimer formation reflects the ability of an excited pyrene molecule to move through oil-rich domains and interact, during the lifetime of the excited state, with another pyrene molecule in the ground state. As this process is controlled by diffusion, the rate of excimer formation

(26) Sanchez-Rubio, M. Ph.D. Thesis, Centro de Investigacion y Estudios Avanzados, Mexico, 1984.
(27) Selinger, B. K.; Watkins, A. R. *Chem. Phys. Lett.* **1978**, *56*, 99.

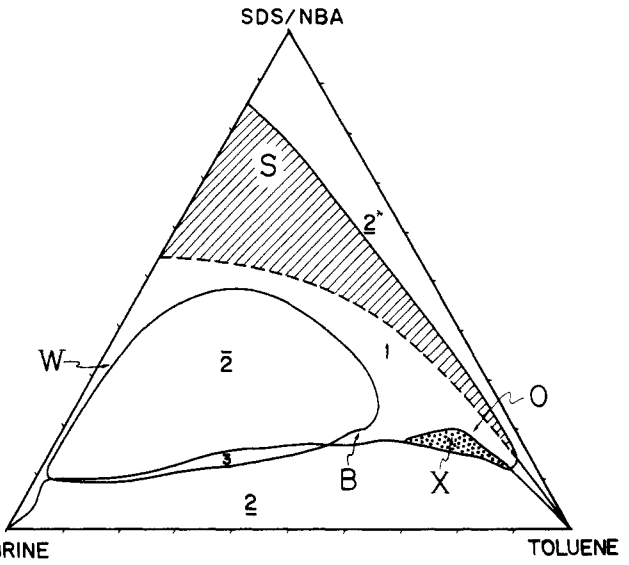

Figure 11. Pseudoternary phase diagram displaying regions with distinct microstructures. Region W: o/w microemulsion. Region O: w/o microemulsion. Region B: bicontinuous microemulsion. Region S (hatched area): excluded region for droplets. Region X: unknown.

will vary inversely with the viscosity of the medium. Moreover, the probability of excimer formation depends on the size of the oil domains as well as on pyrene concentration. Thus, in water-continuous microemulsions, because the diffusion of water-insoluble pyrene molecules is restricted, excimer formation should be low compared to that in pure oil having the same pyrene concentration. Conversely, excimer formation in an oil-continuous microemulsion should be similar to that measured in pure oil.

While conductivity and pyrene fluorescence measure the transport properties of the water and oil domains, QLS provides information on the size and interactions of these domains. QLS measures the growth and decay of refractive index fluctuations of wavelengths $2\pi/q$. The collective diffusion coefficient of domains is measured since $2\pi/q$ ranges from 2000 to 6000 Å in our experiments, a length much greater than the interdomain spacing. As mentioned above, the measured diffusion coefficient, D_{app}, is equal to D_0 in the absence of interactions. As the concentration of particles increases D_{app} is related to D_0[28-30] as

$$D_{app} = \frac{D_0}{S(q)}[1 + A(q)C]$$

Here $S(q)$ is the structure factor that depends on thermodynamic interactions, $A(q)$ is a hydrodynamic interaction term, and C is the average concentration of particles. C is difficult to define in concentrated microemulsions and is meaningless in bicontinuous ones. However, since we found little dependence of D_{app} on q (see Figure 6), we simply define a characteristic length $\xi \sim D_{app}^{-1}$ as above. At low concentrations, $\xi \sim R_h$. The behavior of $S(q)$ and $A(q)$ in microemulsions containing higher concentrations of droplets has been explored.[31]

The following discussion shows there are distinct regions where different structures exist (Figure 11).

Region S. The absence of a significant QLS signal indicates that there is a large zone of the phase diagram (hatched region on Figure 11) where the various components coexist in one transparent, fluid phase without forming micellar-like aggregates (i.e., there is a small or immeasurable ξ). A similar region was reported by Bellocq and Fourche[22] for two salt-free surfactant–alcohol–oil–water systems. Our results of high electrical conductivity and small correlation lengths are consistent with the microemulsion model of Bothorel et al.,[32] based on geometrical considerations, in which a certain region of the system cannot be described either by w/o or o/w droplets or micelles since the filling coefficient of both types of micelles would be higher than the random close sphere packing. In this excluded region for droplets, the system probably consists of small hydrated soap aggregates solvated by alcohol dispersed in an oleic (1-butanol plus toluene) medium. Although a lamellar structure was identified elsewhere by electron microscopy in the upper corner of the one-phase region of the SDS–NBA–toluene–water (no salt) system, the low viscosities detected (Figure 3) and the absence of scattered light rule out such structure in the system with salt investigated here.

Region W. In the region W (Figure 11) where the water-to-oil ratio is much greater than one, microemulsions are highly conducting (Figure 2) so they must be water continuous. Preliminary results show that excimer formation (as measured by the ratio I^{466}/I^{395}) is an order of magnitude smaller than that measured in pure toluene. This result suggests that the oil in the microemulsion is restricted to small domains. Moreover, the q independent characteristic sizes from QLS (Figure 7) are consistent with the presence of micellar structures. Thus, the conclusion is that microemulsions in region W are aqueous solutions of oil-swollen micelles.

Region O. In region O (Figure 11), the ratio of water to oil is less than one. Microemulsion conductivity is four orders of magnitude smaller than in region W (see Figure 2), and the ratio I^{466}/I^{395} (see Figure 8) is comparable to that measured in pure toluene. In addition, characteristic sizes (ξ) are q independent and are consistent with the dimensions associated with w/o micellar structures (Figures 4–6).

Quantitative determination of micelle size depends on understanding the influence of interparticle interactions on the QLS signal. The interactions between w/o micelles have been investigated by Cazabat and Langevin.[33] They found that micelles interact primarily with hard-sphere repulsions, but also with small attractive interactions which increase near phase boundaries. The presence of salt reduces these attractive interactions.[34] Therefore, in the samples studied here, away from the 2 phase boundary (and at low ϕ_w), interactions will be small and we expect $\xi = R_h$. Thus, all the data are consistent with the picture of the w/o microemulsions as oleic solutions of inverted micelles swollen with water.

Region X. Near the 2 phase boundary we label a region X. This region is roughly defined by the onset of increasing conductivity and of rapid growth in ξ with increasing ϕ_T along paths II to V (Figures 5 and 10). The divergence of ξ suggests that critical fluctuations dominate the structure. However, the observed q dependence of $1/D_{app}$ in this region is opposite to that predicted by Kawasaki's theory.[35] Thus the signal is not due to critical fluctuations. A similar observation has been made by Guest and Langevin[36] for a different microemulsion system.

The structure in this region is difficult to decipher. The high conductivity could be explained by the presence of strong attractions between w/o micelles (i.e., the formation of chains of droplets) or by an equilibrium between w/o micelles and highly conductive smaller aggregates dispersed in an oleic medium. The large ξ observed could be related to attractive interactions or to the oil domain size of a rhombododecahedral (RDH) structure suggested previously.[19,37] This kind of face-centered cubic lattice allows a connected aqueous phase at extremely low water content ($\phi_w \sim 0.04$). The data are inconclusive, however, as to the structure in region X.

Region B. In region B (Figure 10), where the volume ratio of water to oil is close to one, conductance, fluorescence, and QLS measurements were taken along several dilution paths (lines 1 to 4) that approach the three-phase region. At low ratios of water

(28) Ackerson, B. J. *J. Chem. Phys.* **1976**, *64*, 242.
(29) Felderhof, B. U. *J. Phys. A* **1978**, *11*, 929.
(30) Fijnaut, H. M. *J. Chem. Phys.* **1981**, *74*, 6857.
(31) Chang, N. J.; Kaler, E. W. *Langmuir* **1986**, *2*, 184.
(32) Bothorel, P.; Biais, J.; Clin, B.; Lalanne, P.; Maelstaf, P. *C. R. Acad. Sci. (Paris), Ser. C* **1979**, *289C*, 409.
(33) Cazabat, A. M.; Langevin, D. *J. Chem. Phys.* **1981**, *76*, 3148.
(34) Bedwell, B.; Gulari, E. *J. Colloid Interface Sci.* **1984**, *102*, 88.
(35) Kawasaki, K. *Phys. Rev. A* **1970**, *1*, 1750.
(36) Guest, D.; Langevin, D. *J. Colloid Interface Sci.* **1986**, *112*, 208.
(37) Chen, S. J.; Evans, D. F.; Ninham, B. W.; Mitchell, D J.; Blum, F. D.; Pickup, S. *J. Phys. Chem.* **1986**, *90*, 842.

to oil (small ϕ_w), the water in the microemulsion is restricted and the oil is continuous: conductivity is extremely low (2 $\mu S \cdot cm^{-1}$), the characteristic size is small ($\xi \sim 30$ Å), and the excimer-to-monomer emission ratio, I^{466}/I^{395}, is similar to that in pure oil (Figure 5). As these microemulsions are diluted with brine, the conductivity rises steeply for ϕ_w above the percolation threshold (Figure 9) and suggests a transition from a nonconducting to a conducting structure. Concurrently, the ratio I^{466}/I^{395} decreases as brine is added to the sample (Figure 8). This decrease is sensible since the volume accessible for pyrene diffusion is reduced, and this hinders the formation of excimers. Yet, in the neighborhood of the three-phase region, where conductivity is higher, I^{466}/I^{395} increases again along lines 2 and 3 suggesting a larger accessible volume or larger oil connectivity through which pyrene molecules can diffuse.

It is worth mentioning that I^{466}/I^{395} is also affected by viscosity as well as by the lifetime of the excited state. However, it is unlikely that either of these factors is responsible for the observed changes: viscosity does not change significantly along the chosen dilution lines (Figure 3) and the pyrene lifetimes measured at low concentrations are almost identical for all the samples examined. We defer discussion of the analysis and interpretation of lifetime data for a subsequent paper.

The conductivity and excimer data collected along the dilution lines indicate that samples near the three-phase region show both high conductance and pyrene mobility; in other words, both oil and water connectivity. The values of ξ measured with QLS along paths 1 to 4 are consistent with the proposed structure for several reasons. First, for small ϕ_w, ξ, which in this case corresponds to the radius of the droplet, increases linearly with ϕ_w and decreases as surfactant is added. These are the results expected if the microemulsion contains a population of droplets coated by surfactant, and if the partitioning of alcohol between the droplets and the oleic continuum is constant. Above the percolation threshold, the different surfactant concentrations in the solutions along lines 1 through 3 dictate that the domain sizes (which no longer increase in direct portion to ϕ_w) are different, i.e., they are larger along line 3 than along line 1. These domains are channels of water, and they provide the means of electrical conductivity. Thus, at a fixed ϕ_w, the conductivity increases as the compositions of the samples move from line 1 to line 4. Geometry dictates that large domains are separated by large distances. This means that I^{466}/I^{395}—the measure of pyrene mobility—should also increase above the percolation threshold more rapidly along line 3 than along 2 or 1 as is observed (Figure 8). The data along line 1 are all consistent with the growth of droplets without the formation of long-lived bicontinuous structures. Above the percolation thresholds along lines 2 and 3, bicontinuous structures exist.

The final observation is that both conductivity and QLS measurements along lines I through V can be explained in terms of the different structural regions proposed above. Thus, the continuous increase in $1/D_{app}$ as the volume fraction of toluene increases (Figure 5) suggest that droplets are organizing as the amount of toluene increases and that, as the phase boundary approaches, the characteristic length grows. The scattering from samples with larger characteristic lengths are q dependent (Figure 6). The conductivity minimum is probably due to the formation of a w/o microemulsion followed by a transition to a water continuous one (region X); although there is a possibility that as ϕ_T increases a competition for the surfactant between the droplets (poor conductors) and monomer in solution (good conductors) could explain the conductivity minimum.

In summary, using a battery of techniques we were able to identify several microemulsion microstructures in the one-phase region of the SDS/NBA/toluene/2.5 wt % NaCl brine system defined by a constant alcohol/surfactant weight ratio of 2. Our results agree with three types of microemulsion structures: an aqueous solution of oil-swollen micelles at high water-to-oil ratios; an oleic (toluene plus alcohol) solution of inverted swollen micelles with water at low water-to-oil ratios; and a bicontinuous interpenetrating network of oil and water domains separated by surfactant-rich layers. We also found a large excluded region for droplets where small hydrated surfactant aggregates are dispersed in an oleic medium and a small region where the structure is puzzling; here microemulsions with low water content appear to be water continuous.

Acknowledgment. This work was supported by the NSF under Grants CPE-8351179 and INT-8502390, and by CONACYT under Grant PCCBBNA-023157.

Registry No. SDS, 151-21-3; NaCl, 7647-14-5; 1-butanol, 71-36-3; toluene, 108-88-3.